



Published in final edited form as:

Soft Matter. 2011 ; 2011(7): 1656–1659. doi:10.1039/C0SM01131B.

Facile One-Pot Synthesis of Polymer-Phospholipid Composite Microbubbles with Enhanced Drug Loading Capacity for Ultrasound-Triggered Therapy

Matthew A. Nakatsuka^a, Joo Hye Lee^a, Emi Nakayama^a, Albert M. Hung^a, Mark J. Hsu^b, Robert F. Mattrey^c, Sadik C. Esener^{a,b,*}, Jennifer N. Cha^{a,*}, and Andrew P. Goodwin^{a,*}

^aUniversity of California, San Diego, Department of Nanoengineering, 9500 Gilman Dr. #0048, La Jolla, CA 92093, USA

^bUniversity of California, San Diego, Department of Electrical and Computer Engineering, 9500 Gilman Dr. #0407, La Jolla, CA 92093, USA

^cUniversity of California, San Diego, Department of Radiology, 410 Dickinson St., San Diego, CA 92103

Abstract

This paper reports the one-pot synthesis of perfluorocarbon microbubbles with crosslinked shells of poly(acrylic acid) and phospholipid that boast excellent ultrasound contrast enhancement, enhanced loading capacity, and the ability to retain or release their contents through variation in the level of ultrasound exposure.

Theranostics, or agents that can both be tracked through non-invasive imaging and induce therapy selectively at a diseased site, are highly desired for simultaneous diagnosis and treatment of many diseases. These tools would allow a clinician to obtain detailed information about a potentially diseased site, locate the material within the patient, and induce therapy at that specific location if desired. The ideal theranostic can be imaged non-invasively at low concentrations deep within most tissues, remain benign under imaging conditions, and be loaded with enough drug molecules to impact a diseased site upon activation. In this paper, we describe a new type of ultrasound theranostic microbubbles stabilized by composite shells of polymer and phospholipid. These microbubbles show similar ultrasound enhancement properties to standard microbubble formulations, but possess greatly improved drug loading capabilities over lipid-shelled bubbles. Furthermore, these microbubbles are synthesized very easily in a one-pot reaction.

While many energy sources have been considered for externally-triggered drug release, ultrasound possesses a combination of benefits unmatched by other modalities both for imaging and as a means to trigger drug release from outside the patient. First, ultrasound can pass through most tissues with relatively little attenuation or scattering and can be focused down to *ca.* 1 mm³ within a patient with substantial penetration depths at a range of intensities. Furthermore, ultrasound is generally safe and imaging can be performed with inexpensive, portable equipment found at most hospitals and clinics. As a pressure wave, ultrasound is best able to react with a drug carrier by inducing mechanical stress on the structure.^[1] Since ultrasound energy is both deposited and reflected at interfaces of media

agoodwin@ucsd.edu, jencia@ucsd.edu, sesener@ucsd.edu.

[†]Electronic Supplementary Information (ESI) available: Experimental details, microbubble size distributions, FACS data, higher intensity ultrasound attenuation data. See DOI: 10.1039/b000000x/

with large differences in compressibility, microbubbles are very efficient at reflecting incident ultrasound, and when insonated at their resonance frequency with sufficient power they can generate selectively-detectable harmonic signals through oscillation at harmonic and subharmonic modes.^[2, 3] In addition, at larger ultrasound intensities the microbubbles may cavitate violently, generating shock waves that perforate cell membranes and allow macromolecules such as DNA, proteins, or polymers to pass directly into the cytoplasm.^[4]

Despite the advantages of microbubbles as imaging contrast agents, the large, fluorinated gas core limits the amount of drug that can be loaded into each bubble and thus their effectiveness as drug delivery vehicles. Most microbubbles are stabilized by a monolayer of phospholipids that can hold only a thin layer of drugs.^[5] While functional groups may be added to the structure of poly(ethylene glycol)-based or albumin-based bubbles, the necessary covalent conjugation of drugs requires an additional mechanism to release the drug in its active form.^[6] The best option therefore appears to be to create a shell that contains excess drug molecules that can potentially be ejected into the surroundings. In initial attempts, drugs were formulated in an oil layer surrounding the bubbles,^[7] but the presence of the oil reduced the ability of the microbubble to cause drug release.^[8] Other ultrasound contrast agents like acoustically active liposomes possess poorer echogenicity and are less efficient contrast agents.^[9] In response to these challenges, some research groups have worked on attaching liposomes to the outside of the microbubbles for additional drug storage via biotin-streptavidin interactions,^[10] while others have used a layer-by-layer technique to adsorb polymers and DNA for gene delivery^[11] using postformulation modification. Finally, microfluidics has also been used to create both shelled microbubbles with layers of drug encapsulation.^[12]

Here, we report a novel method to create microbubbles with high drug loading capacity through the co-mixing of lipids and a polymer that has reversible affinities for the lipid headgroup. The key component for the successful synthesis of the polymer-lipid microbubble shells is poly(acrylic acid) (PAA), which binds to phosphocholine headgroups below its pKa of 4.5 but has little affinity at physiological pH.^[13] When simply mixed with preformed liposomes at acidic pH, PAA is thought to either intercalate into the alkyl tail groups or cause ripples in the bilayer, destabilizing the assembly and causing liposome rupture.^[13] However, if the PAA and lipid are first mixed together at acidic pH to promote polymer-lipid association and crosslinked into place, the resultant assemblies are stable to biological conditions. Thus our strategy is to mix partially thiolated PAA with a phospholipid suspension, sonicate the mixture under perfluorocarbon gas to form the microbubbles, and then induce disulfide crosslinking to generate microbubbles that each possess a thick stable polymer-lipid shell which would enable high drug loading.

First, PAA ($M_w \sim 5000$ Da) was partially functionalized with cysteamine to add thiol groups and then labeled with a maleimidyl fluorescein isothiocyanate derivative (FITC; Fig. 1). The polymer was combined with a premade suspension of 1,2-distearoyl-*sn*-glycerco-3-phosphocholine (DSPC) in pH 3.4 acetate buffered saline (ABS). Perfluorobutane (PFB) was flowed into the headspace above the suspension and the mixture was probe sonicated at the gas-liquid interface for 10 s, forming the microbubbles. The microbubbles were then centrifuged at 300 g for 3 min to float the bubbles, followed by removal of the supernatant and replacement with ABS. The microbubbles were exposed to 10 mM hydrogen peroxide for 20 min to form disulfide bridges, followed by centrifuge washing three times with PBS.^[14] The gas-filled microbubbles are easily visualized by transmission optical microscopy due to the large difference refractive index compared to the surrounding buffer, and the polymer is identified through fluorescence microscopy; the overlay of these images confirms the co-localization of the polymer to the microbubble surface (Fig. 1). During the synthesis at pH 3.4, while the protonated PAA alone can also stabilize larger bubbles, these are not stable at

neutral pH (data not shown). Microbubbles formed with DSPC alone are stable but are formed at a yield of $6 \pm 1 \times 10^7$ microbubbles/mL as compared to $7 \pm 1 \times 10^7$ microbubbles/mL with PAA and DSPC (see Supporting Information). This increase in yield is most likely due to the steric and electronic repulsion between anionic PAA chains that resist coalescence and promote bubble stability. Irrespective of PAA addition, the bubble size means and distributions are about the same, with average bubble diameters of $2.4 \pm 0.8 \mu\text{m}$ and $2.5 \pm 0.8 \mu\text{m}$, respectively (see Supporting Information). This microbubble size range similar to commercial formulations and thus is appropriate for in vivo imaging.^[3]

The characterization of the composition of the bubbles indicated the shell was comprised of both PAA-SH and DSPC. First, the microbubbles were washed of excess polymer and lipid and examined by NMR spectroscopy, which showed the clear presence of the PAA-SH-FITC in the washed microbubble sample (see Supporting Information). Next, attempts were made to characterize the shell by transmission electron microscopy (TEM), but the microbubbles proved unstable to the conditions of the TEM. To approximate the shell on a more stable substrate, the same DSPC/PAA-SH-FITC shell was formed on the surface of a silica microparticle. The microparticle was first rendered hydrophobic through reaction with N,N,N',N',N',N'-hexamethyldisilazane (HMDS), and then the film was formed on the microparticle through sonication in the presence of DSPC and PAA-SH-FITC and hydrogen peroxide oxidation. The particles containing the DSPC/PAA-SH-FITC shell were stained with uranyl acetate to stain primarily the PAA in the presence of the lipids. As shown in Fig. 2, the film appears to be 6–9 nm, although it is difficult to draw direct conclusions about substructure from these images alone. However, since lipids are known to form monolayers on the microbubble surface,^[15] the shell appears to contain a composite of phospholipid and polymer that may be used to encapsulate drug.

The microbubbles must reflect ultrasound efficiently so that their pharmacokinetics can be tracked within the patient. Thus it was important for the microbubbles to retain their ultrasound properties despite the addition of the crosslinked shell. The standard of comparison for these studies were microbubbles formulated to be similar to Definity®, a common lipid-shelled microbubble that contains a stabilizing layer of poly(ethylene glycol) conjugated to a lipid. For these studies, microbubbles were formulated with the same mass ratios of DPPC, DPPA, and DSPC-mPEG corresponding to Definity®. The ultrasound reflectivity of these microbubbles were measured in vitro in an agar phantom. As shown in Fig. 3e, the resonance frequency of the microbubbles shifts only slightly from 1.5 MHz, consistent with Definity at this frequency range,^[16] to 1.7 MHz. This slight increase in shell thickness and rigidity due to crosslinking is consistent with theoretical descriptions.^[2]

Next, suspensions of microbubbles at 100 fM were added to an agar phantom and pulsed at 2.25 MHz at diagnostic pressures ranging from 24 kPa to 89 kPa (Fig. 3a–d). The backscattered signal of the microbubbles is slightly poorer at 24 kPa, about the same for 43 kPa and 69 kPa, and slightly greater at 89 kPa. We attribute the signal dampening at 24 kPa to the slight reduction in bubble compressibility caused by the presence of the shell, a change which would be observed best at incident pressures insufficient to cause size fluctuations in the stiffer bubbles. However, this same polymer shell provides added stability, and so the sharp decrease at the beginning of the insonation at 89 kPa is most likely due to the destruction of bubbles with resonance frequencies near that of the incident pulse (Fig. 2d). Thus lower diagnostic pressures may be used to image the bubbles without destroying them. When the ultrasound pressure is increased to 89 kPa, also within diagnostic range, the microbubbles degrade steadily. When the microbubbles were pulsed at 357 kPa, still within diagnostic range, they degrade quite readily, losing over half of their attenuation within one minute (see Supporting Information).

To determine the microbubbles' ability to act as drug carriers, Rhodamine B was used as a model lipophilic drug. The dye was mixed into the lipid mixture prior to formulation and prepared as before, producing bubbles that show much stronger red fluorescence than their lipid-only labeled counterparts (Fig. 4). According to flow cytometry studies (Supplementary Information), the bubbles with PAA-SH showed an average of 3-fold greater fluorescence than those without PAA. In addition, when Rhodamine B was formulated into DPPC/DPPA/DSPE-mPEG, little fluorescence from the Rhodamine B could be observed on the bubbles. Fluorescence microscopy also shows that the red fluorescence of the dye is co-localized with the green fluorescence of the PAA-SH-FITC, even in areas of uneven polymer coating. The increase in dye loading may be due to formation of lipid networks that can be filled with organic molecules or also to electrostatic binding between Rhodamine B and the PAA. If the latter case is true, the presence of the negatively charged PAA should be sufficient to bind drugs containing cationic groups, such as doxorubicin.^[17] If neither hydrophobicity or positive charge is present for a potential drug, the PAA may be appended further to include additional functional groups that show affinity for such drugs. Regardless, it is clear that the increase in dye loading in the study shows that a multicomponent shell is able to load larger amounts of cargo than a simple lipid shell.

In conclusion, we have shown that stable phospholipid-polymer microbubbles with enhanced drug loading can be made in a simple one-pot synthesis. These microbubbles are effective ultrasound contrast agents that also showed improved echogenicity as well as overall stability compared to lipid-only bubbles. Furthermore, because these DSPC/PAA-SH microbubbles appear to possess cross-linked composites of lipid and polymer, they are able to load much more dye than other lipid-stabilized microbubbles, which should translate well to future drug loading studies. Finally, while the polymer-lipid microbubbles are stable to normal imaging conditions, the bubbles degrade at increased ultrasound pressures that are still within the diagnostic range, enabling the future use of these structures as theranostic agents that can be tracked within a patient and externally triggered to release high amounts of drug at a specified site of inflammation.

Supplementary Material

Refer to Web version on PubMed Central for supplementary material.

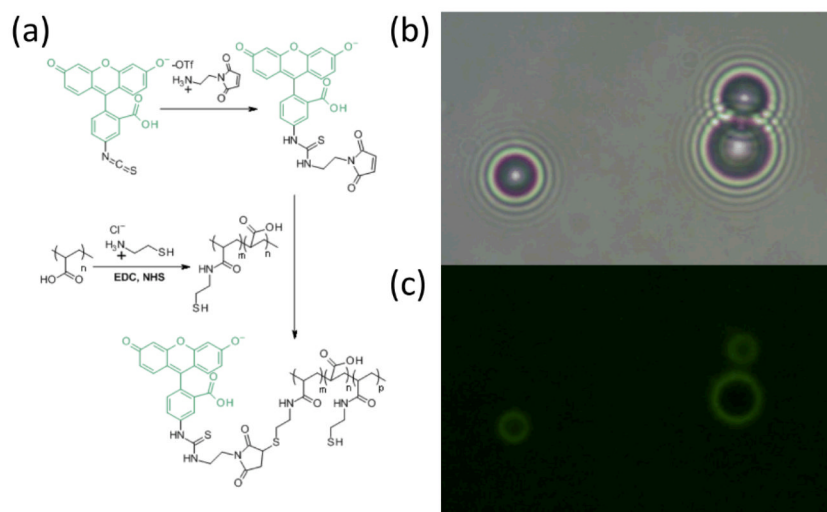
Acknowledgments

This work was supported by UCSD startup funds (J. N. C.), U54CA119335, and P50CA128346. A. P. G. is a recipient of a UCSD Cancer Therapeutics Training Program NIH Postdoctoral Fellowship (T32CA121938) and a Pathway to Independence Award in Cancer Nanotechnology (K99CA135935). M. A. N. is the recipient of a UCSD Cal-RA Fellowship. The authors thank Dr. Davorka Messmer and Dr. Ana Sanchez for help with FACS.

Notes and references

1. Berkowski KL, Potisek SL, Hickenboth CR, Moore JS. *Macromol.* 2005; 38:8975–8978. Hickenboth CR, Moore JS, White SR, Sottos NR, Baudry J, Wilson SR. *Nature.* 2007; 446:423–427. [PubMed: 17377579]
2. Church CC. *J Acoust Soc Am.* 1995; 97:1510–1521. Hoff L, Sontum PC, Hovem JM. *J Acoust Soc Am.* 2000; 107:2272–2280. [PubMed: 10790053]
3. Schutt EG, Klein DH, Mattrey RM, Riess JG. *Angew Chem Int Ed.* 2003; 42:3218–3235.
4. Ferrara K, Pollard R, Borden M. *Annu Rev Biomed Eng.* 2007; 9:415–447. [PubMed: 17651012]
5. Lentacker I, Geers B, Demeester J, De Smedt SC, Sanders NN. *Mol Ther.* 2010; 18:101–108. [PubMed: 19623162] Treat LH, McDannold N, Vykhodtseva N, Zhang Y, Tam K, Hynynen K. *Int J Cancer.* 2007; 121:901–907. [PubMed: 17437269]
6. Klibanov AL. *Bioconjugate Chem.* 2005; 16:9–17.

7. Unger EC, McCreery TP, Sweitzer RH, Caldwell VE, Wu YQ. *Invest Radiol.* 1998; 33:886–892. [PubMed: 9851823]
8. Lentacker I, De Smedt SC, Sanders NN. *Soft Matter.* 2009; 5:2161–2170.
9. Hernot S, Klibanov AL. *Adv Drug Deliv Rev.* 2008; 60:1153–1166. [PubMed: 18486268] Ophir J, Parker KJ. *Ultrasound in Medicine and Biology.* 1989; 15:319–333. [PubMed: 2669297] Wheatley MA, Lathia JD, Oum KL. *Biomacromol.* 2007; 8:516–522.
10. Kheiroloom A, Dayton PA, Lum AF, Little E, Paoli EE, Zheng H, Ferrara KW. *J Control Release.* 2007; 118:275–284. [PubMed: 17300849]
11. Becker AL, Zelikin AN, Johnston APR, Caruso F. *Langmuir.* 2009; 25:14079–14085. [PubMed: 20560555]
12. Hettiarachchi K, Lee AP. *J Colloid Interf Sci.* 2010; 344:521–527. Hettiarachchi K, Lee AP, Zhang S, Feingold S, Dayton PA. *Biotechnol Progr.* 2009; 25:938–945. Talu E, Hettiarachchi K, Zhao S, Powell RL, Lee AP, Longo ML, Dayton PA. *Molecular Imaging.* 2007; 6:384–392. [PubMed: 18053409]
13. Seki K, Tirrell DA. *Macromol.* 1984; 17:1692–1698. Thomas JL, Tirrell DA. *Acc Chem Res.* 1992; 25:336–342. Fujiwara M, Grubbs RH, Baldeschwieler JD. *J Colloid Interf Sci.* 1997; 185:210–216.
14. Zelikin AN, Li Q, Caruso F. *Chem Mater.* 2008; 20:2655–2661. Zelikin AN, Quinn JF, Caruso F. *Biomacromol.* 2006; 7:27–30.
15. Borden MA, Martinez GV, Ricker J, Tsvetkova N, Longo M, Gillies RJ, Dayton PA, Ferrara KW. *Langmuir.* 2006; 22:4291–4297. [PubMed: 16618177] Ferrara KW, Borden MA, Zhang H. *Acc Chem Res.* 2009; 42:881–892. [PubMed: 19552457]
16. Chatterjee D, Sarkar K, Jain P, Schreppler NE. *Ultrasound in Medicine and Biology.* 2005; 31:781–786. [PubMed: 15936494]
17. Tinkov S, Winter G, Coester C, Bekerredjian R. *J Control Release.* 2010; 143:143–150. [PubMed: 20060861]

**Figure 1.**

(a) Synthesis of FITC-labeled thiolated poly(acrylic acid). Thiol groups were functionalized on 11% of monomer units. (b) Bright field transmission image of microbubbles comprised of DSPC and PAA-SH-FITC, showing location of perfluorobutane gas. (c) Green fluorescence image of same, showing PAA-SH-FITC.

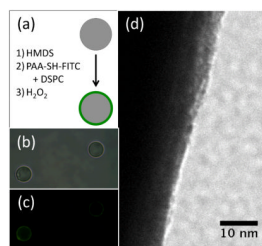


Figure 2. Examination of model shell on silica microparticles by TEM. (a) Schematic of hydrophobic functionalization of silica and formation of shell. (b) Bright field image of silica particles containing silica with shells. (c) Green fluorescence image of silica particles containing silica with shells. (d) TEM image of PAA-DSPC formed on hydrophobic silica microparticle. Shell is approximately 6–9 nm thick.

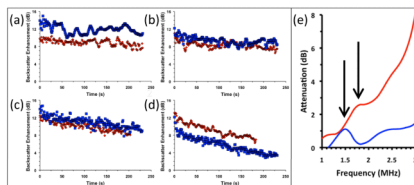


Figure 3. Ultrasound characterization of microbubbles with different polymer shells (blue = PEG-DSPE, red = PAA-SH-FITC). (a–d): Backscatter of impulse at 2.25 MHz (100 kHz repetition rate) was measured in an agar phantom at RT. Signal is expressed as enhancement over PBS blank. Backscatter measurements at (a) 24 kPa, (b) 43 kPa, (c) 69 kPa, and (d) 89 kPa peak pressure vs. time. (e): Acoustic attenuation spectra of microbubbles with one sine wave at 2.25 MHz. Attenuation is expressed as loss of through signal compared to PBS blank.

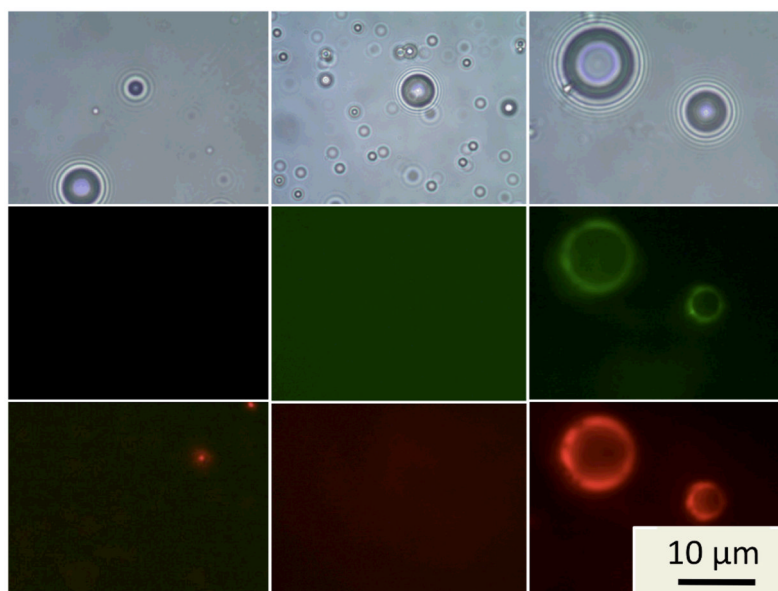


Figure 4. Comparison of Rhodamine B loading for microbubbles with DSPC only (left), DPPC/DPPA/DSPE-mPEG (center), and with DSPC/PAA-SH-FITC (right). Top images: bright field transmission mode. Middle images: Green fluorescence show the presence of PAA-SH-FITC. Bottom images: Red fluorescence shows the presence of Rhodamine B. The exposure time for lipid-only and mPEG bubbles is 16 times greater than for PAA bubbles, confirming the great difference in Rhodamine B loading.